



Drag Prediction in the Near Wake of a Circular Cylinder based on DPIV Data

O. Son[†] and O. Cetiner

Department of Astronautical Engineering, Istanbul Technical University, Istanbul, 34469, Turkey

[†]Corresponding Author Email: sono@itu.edu.tr

(Received February 1, 2015; accepted September 22, 2015)

ABSTRACT

This study focuses on drag prediction in the near-wake of a circular cylinder by use of mean velocity profiles and discusses the closest location where a wake survey would yield an accurate result. Although the investigation considers both the mean and fluctuating velocities, the main focus is on the mean momentum deficit which should be handled properly beyond a critical distance. Digital Particle Image Velocimetry (DPIV) experiments are performed in a Reynolds number range of 100 to 1250. Wake characteristics such as vortex formation length (L) and wake width (t) are determined and their relations to drag prediction are presented. Drag coefficients determined by momentum deficit formula are found to be in good agreement with experimental and numerical literature data in present Reynolds number regime.

Keywords: Circular cylinder; Drag prediction; DPIV; Momentum deficit.

NOMENCLATURE

C_d	drag coefficient	t	wake width
$C_{d,max}$	maximum value of drag coefficient	U_∞	freestream velocity
$C_{d,mean}$	average value of drag coefficient	u'	streamwise root mean square (rms) velocity
D	cylinder diameter	v'	cross-stream root mean square (rms) velocity
h	visualization height	δ^*	displacement thickness
I_1	momentum deficit integral	ν	kinematic viscosity
I_2	turbulent fluctuations integral		
L	vortex formation length		
Re	Reynolds number $Re=(U_\infty \times D)/\nu$		

1. INTRODUCTION

Both the flow around circular cylinders and accurate prediction of drag has received extensive interest in the past (Antonia and Rajagopalan 1990). Formulations are presented to determine instantaneous forces on different bodies by means of instantaneous velocity and its derivatives. These expressions are particularly useful for experimental techniques like Digital Particle Image Velocimetry (DPIV) which provides spatial and temporal distribution of velocity fields. It is also an attractive way to obtain load data without the use of surface instrumentation or external balance mechanism. Recent efforts on velocity-force relation are in the field of DPIV-based pressure measurements, which introduces novel diagnostic methodology for determining the instantaneous flow field pressure (Oudheusden 2013). Despite all the experience gained with DPIV-based pressure and loads

determination, further investigation is still required to discover the possibilities and limitations of these methods.

In literature, there are various approaches to determine the drag coefficient by using mean velocity profiles and fluctuation terms. One of these methods described by Dimotakis (1977) and recently used in study of Wen *et al.* (2004) is given as;

$$C_d = \frac{2h/D}{(1 - (\frac{\delta^*}{h})^2)} \left[\int_0^1 \frac{U}{U_\infty} \left(1 - \frac{U}{U_\infty}\right) d\eta - \int_0^1 \frac{u'^2 - v'^2}{U_\infty^2} d\eta + \frac{1}{2} \left(\frac{\delta^*}{h}\right)^2 \right] \quad (1)$$

Where u' and v' are streamwise and cross-stream root mean square (rms) velocities, h is the visualization height and δ^* is the displacement thickness. A

similar concept is lately applied by Bohl and Koochesfahani (2009) to determine force coefficients for an oscillating airfoil.

Another method for estimation of drag coefficient is described by Townsend (1980) and verified for the wake of a circular cylinder in the study of Antonia and Rajagopalan (1990). The formula of this estimation method is given below and referenced in various recent studies, e.g., comparison of fluid forces of an airfoil (Zhou *et al.* 2011), drag calculations of a flat plate at various angles of attack (Sharma and Deshpande 2012), drag estimations of circular cylinder with synthetic jet (Feng and Wang 2012), symmetric vortex shedding in the wake of a cylinder (Konstantinidis and Balabani 2007), drag reduction of square cylinders with cut-corners (He *et al.* 2014), characterization of the effect of flow-control excitation from synthetic jet actuators on airfoil drag (Goodfellow *et al.* 2012) and drag reduction of hydrophobized sand on cylinders (Brennan *et al.* 2014).

$$C_d = 2 \int_{-\infty}^{+\infty} \frac{U}{U_\infty} \left(1 - \frac{U}{U_\infty}\right) d\eta + 2 \int_{-\infty}^{+\infty} \frac{v'^2 - u'^2}{U_\infty^2} d\eta \quad (2)$$

In this formulation, the first term which will be referred to as I_1 henceforth is the momentum deficit (momentum thickness) of the time averaged flow field and the second term which will be referred to as I_2 henceforth is the contribution of the streamwise u' and cross-stream v' turbulent fluctuations. The momentum equation, namely the first term I_1 , is sufficient to calculate the drag coefficient using a profile of mean velocity in far wake where the static pressure is nearly recovered to its free-stream value. However, in the near wake region, the negative pressure gradient term needs to be accounted for and as Antonia and Rajagopalan (1990) suggest, this is actually included in the formulation by the Reynolds normal stress terms, namely the second term I_2 .

Antonia and Rajagopalan (1990) claim that if the velocity profiles are taken 30 diameters away from the cylinder, the contribution of the second term can be neglected. However, in the measurements systems such as DPIV, the visualized region is limited. Therefore, investigation of the near wake region with regard to momentum deficit and turbulence terms is important. In this study, calculations are made in the wake of a circular cylinder of diameter $D=1$ cm, over the range of $0 < x/D < 13.6D$. Mean velocity and fluctuation terms are determined in the near wake of the circular cylinder from its base at various aforementioned x/D positions using a DPIV system. The integrals I_1 and I_2 are estimated using these velocity profiles and critical regions for an appropriate drag calculation are determined.

2. EXPERIMENTAL SETUP

Experiments are performed in the close-circuit, free-surface, large scale water channel located in the Trisonic Laboratories at the Faculty of Aeronautics

and Astronautics of Istanbul Technical University. The cross-sectional dimensions of the main test section are 1010 mm × 790 mm. The cylinder has a diameter of 1 cm and span of 45 cm; it is immersed in the channel with two end plates on both sides as shown in the Figure 1. Reynolds number ranges from 100 to 1250.

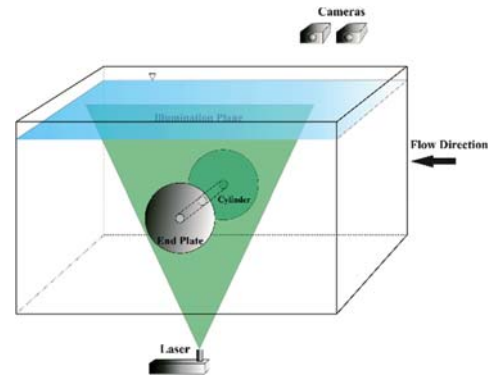


Fig. 1. Experimental Setup.

DPIV technique is used to record flow fields around the cylinder and therefore to analyze the vortical structures, mean velocity profiles and fluctuation terms. The flow is illuminated by a dual cavity Nd: Yag laser (max. 120mJ/pulse) and the water is seeded with silver coated hollow glass spheres with a mean diameter of 10 μm. The velocity fields in the near wake of the circular cylinder are obtained using two 8-bit cameras with 1008 × 1016 pixel resolution, positioned on one side of the water channel. Recorded images are interrogated using a double frame, cross-correlation technique with a window size of 32 × 32 pixels and 50% overlapping in each direction which corresponds to a 1.33 mm × 1.33 mm vector resolution. For each case, 256 vector fields are recorded and averaged to obtain mean velocity fields which are then evaluated for drag prediction analyses. The total velocity uncertainty in the DPIV experiments is less than 2%.

3. RESULTS

Velocity distributions and fluctuation terms are extracted from the processed data and integrals yielding drag coefficient are calculated by means of these velocity profiles. Sample data for Re=500 including mean streamwise velocity (U) contours and streamlines are presented in Figure 2. Wake characteristics such as vortex formation length (L) and wake width (t) definitions are also illustrated in Fig. 2. In the present study, vortex formation length is defined as the distance between cylinder base and the point where mean velocity values are zero on the recirculation bubble. On the other hand, the wake width is defined as the distance between points where the flow reaches 90% of the free stream velocity in upper and lower side of the wake. In our drag coefficient estimations, both of these properties of the wake seem to have significant effects on the results.

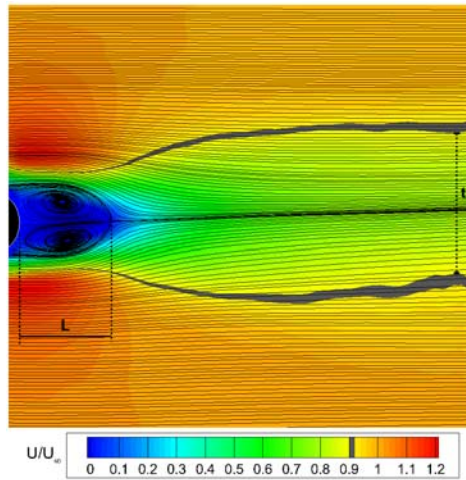


Fig. 2. Vortex formation length (L) and wake width (t) definitions.

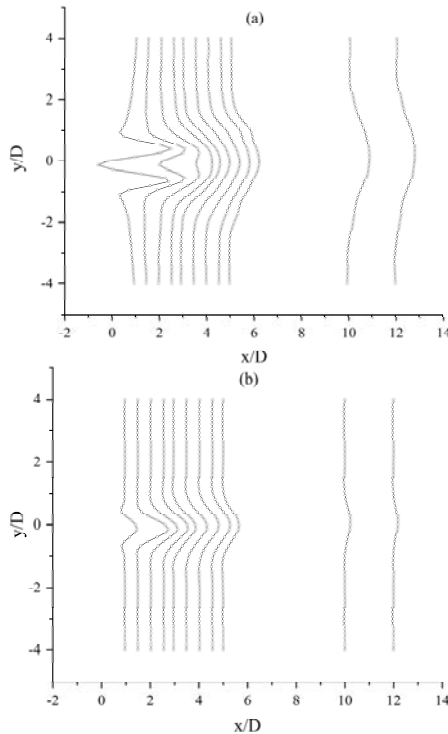


Fig. 3. Variation of C_d integration terms (a) I_1 , and (b) I_2 , with distance at $Re=500$.

One of the questions on drag prediction from velocity profiles is at what distance from the body should we perform integration to determine drag coefficient. To clarify the question, evolution of the integrals I_1 and I_2 along the wake of the cylinder is determined. Figure 3 shows the distribution yielding the term I_1 with respect to the distance from the cylinder base. After the recirculation bubble (for $Re=500$ @ $x/D=1.4$), the distribution yielding momentum integral has some deficit in the recovery region where flow accelerates, until a point where velocity reaches half of the freestream velocity on the centerline. Near that point (for $Re=500$ @

$x/D=2.5$), the value in momentum deficit integral reaches its maximum value on the centerline. Subsequently, integral value I_1 also decreases for increasing x/D . If the integral is undertaken at a location x/D where the centerline velocity does not exceed $0.5 U_\infty$, the distribution will have a local minimum on the centerline and consequently the integral value I_1 will yield a considerably low value causing to seriously underestimate the drag coefficient.

Fluctuation integral term I_2 has a similar distribution in the near wake region as I_1 (Figure 3). This integral also reaches a maximum at a location x/D where the centerline velocity is $0.5 U_\infty$. As x/D increases, contribution of the term I_2 to total drag decreases. According to the study of Antonia and Rajagopalan (1990), at a downstream location around $30D$, I_2 integral value decreases to zero.

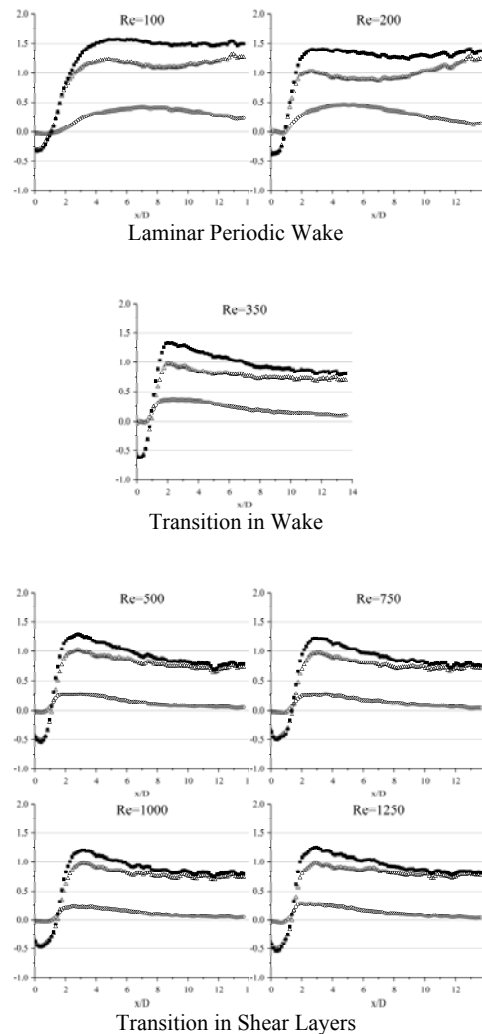


Fig. 4. Drag Coefficient (\blacksquare), I_1 (Δ) and I_2 (\circ) integration terms calculated along the wake.

Classified by Zdravkovich (1997), flow regimes present the epitome of flow states for circular cylinders from laminar to fully turbulent cases. According to these categories, similar distributions

of C_d , I_1 and I_2 within the same group are observed as given in Figure 4. For Reynolds numbers 100 and 200 (“Laminar Periodic Wake Regime”), I_1 integral indicates a diverging progress in our visualization region. This progress is compensated by the decrease of I_2 integral in the same region and eventually constant C_d values are determined. For $Re=350$ (“Transition in Wake Regime”), both I_1 and I_2 increase up to a point, then start to decrease and converge to constant values. The variations have the same behavior for “Transition in Shear Layers” cases corresponding to Reynolds numbers of 500, 750, 1000 and 1250.

Diverging I_1 values for Reynolds numbers of 100 and 200 are related to the wake width characteristics. As shown in the Figure 5, wake widths for Reynolds number of 350 and above converge to a value of $t/D = 1.5 - 2$, whereas there is a continuous increase for Reynolds numbers of 100 and 200.

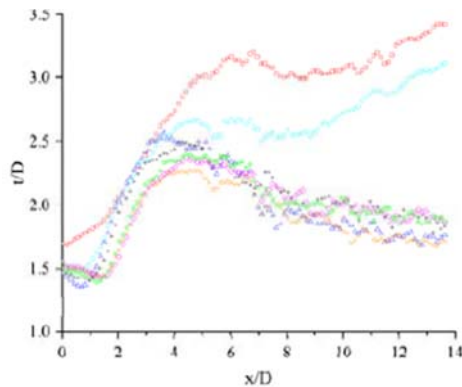


Fig. 5. Wake width for different Reynolds numbers, $Re=100$ (\square), $Re=200$ (\circ), $Re=350$ (Δ), $Re=500$ ($+$), $Re=750$ (\times), $Re=1000$ (\diamond), $Re=1250$ (\star).

It is evident from Figure 4 that the estimated value for the drag coefficient is not constant or does not converge to a constant value based on the location in the near wake. We suggest that the peak value of the drag coefficient $C_{d,max}$ can be used for estimation. This approach will allow more reliable drag comparison for different flow regimes. It will also enable us to make drag estimations in a limited field of view. Besides $C_{d,max}$, we also calculated mean values of drag coefficient ($C_{d,mean}$) for $10 < x/D < 13.6$, where C_d values tend to converge for most of the cases. In Figure 6, the location where we measure the vortex formation length L , $0.5 U_\infty$ and where we calculate $C_{d,max}$ are given with respect to Reynolds number. The region where C_d value is considered for the calculation of a mean value is also shown on the figure as a shaded rectangular box. As stated before, when the recirculation bubble closes, velocity vectors switch from negative to positive marking a zero velocity point on the centerline; and we define the distance from the base of the cylinder to that point as the vortex formation length. Around $Re=300$, vortex pairs have shortest formations and as Reynolds number increases formation length increases. Amongst our investigated Reynolds numbers, $Re=1000$ seems to have the longest

formation length. After the recirculation bubble, the centerline velocity increases in recovery zone and reach $0.5 U_\infty$. This point is critical because of mathematical nature of the integral formula, where integrand of the first integral, I_1 , reaches its maximum (Figure 3) and subsequently highest I_1 integral and high C_d values are obtained. This is the reason why $C_{d,max}$ and $0.5 U_\infty$ positions are quiet close to each other, as seen in Figure 6.

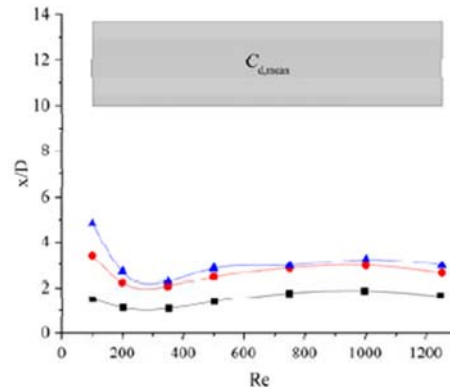


Fig. 6. Vortex formation length (\blacksquare), $0.5 U_\infty$ (\bullet) and $C_{d,max}$ (\blacktriangle) locations.

Vortex formation lengths vary with Reynolds number. The location where we measure $0.5 U_\infty$ and calculate $C_{d,max}$ are affected accordingly. Therefore, as a summary, downstream locations where $C_{d,max}$ are calculated vary with Reynolds number and the location where the centerline velocity reaches $0.5 U_\infty$ defines a lower limit to have accurate estimation results. Before this limit in the streamwise direction and inside the recirculation bubble, the estimations are not reliable.

Estimated drag coefficients in the current study are given in Fig. 7, in comparison with the experimental data of Wieselsberger (1922) and numerical simulation results of Jordan and Fromm (1972), Henderson (1995) and Cao *et al.* (2010). Maximum mean drag coefficient $C_{d,max}$ values are in the band of literature data and follows the trend of experimental ones. It is notable that the maximum mean drag coefficient $C_{d,max}$ values are in a close agreement with the newest data obtained using DNS (Cao *et al.*, 2010). The use of $C_{d,max}$ will allow the experimenter to estimate drag coefficient in the near wake for $1 \leq x/D \leq 5$. Mean drag coefficients obtained using the values for $10 \leq x/D \leq 13.6$, where the effect of fluctuating velocities is lower than near field, result in lower C_d values compared to the data in literature. As the Reynolds number increases, mean drag coefficient estimation improves; however it will not be recommended to be used for the near wake region. Although the formulation used takes into account the variation in pressure, the velocity fluctuation terms are susceptible to the uncertainty in DPIV.

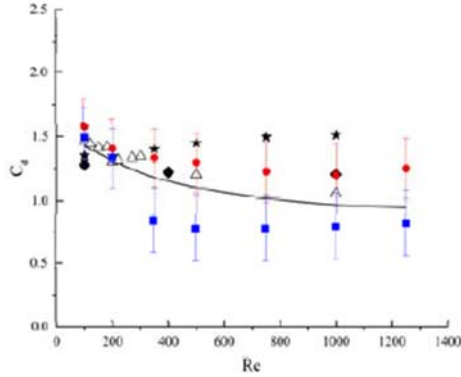


Fig. 7. Drag coefficients in the literature and in the current study, Wieselsberger (—), Jordan and Fromm (●), Henderson (★), Cao et al. (Δ), $C_{d,max}$ (●), $C_{d,mean}$ (■).

Contributions of the I_1 and I_2 integrals to the total drag coefficient $C_{d,max}$ are given in Table 1. In the study of Antonia and Rajagopalan (1990), for a Reynolds number of 5600, at $x/D=5$, I_2 contributes 22% to C_d and this contribution decreases as x/D increases. In our cases, contribution of I_2 is in between 18% to 27% for different Reynolds numbers (Table 1).

Table 1 Estimated drag coefficients and contributions of I_1 and I_2 integrals.

Re	I_1	I_2	$I_1\%$	$I_2\%$	$C_{d,max}$	$C_{d,mean}$
100	1.228	0.350	77.81	22.19	1.578	1.494
200	1.032	0.369	73.67	26.33	1.401	1.327
350	0.963	0.364	72.58	27.42	1.327	0.841
500	1.027	0.268	79.31	20.69	1.294	0.780
750	0.967	0.259	78.87	21.13	1.226	0.780
1000	0.978	0.221	81.58	18.42	1.199	0.797
1250	0.984	0.265	78.80	21.20	1.249	0.819

4. CONCLUSION

Velocity profiles in the near wake of a circular cylinder have been obtained using a 2D2C DPIV system for a Reynolds number range of 100 to 1250. Recently accepted drag coefficient prediction formula in literature is used to determine drag coefficients by using these velocity profiles. Wake properties such as vortex formation length and wake width are also determined and their relation to drag prediction is studied. As a result of analyses, we recommend to use the velocity profiles after the centerline velocity reaches $0.5 U_\infty$, preferably the velocity profile close to this location where a maximum drag coefficient is calculated. This approach yields results in a good agreement with the literature and enables the experimenter to use a limited field of view ($x/D \leq 5$), since the location where the maximum drag coefficient is calculated is about a few vortex formation length distant from the base of the cylinder. It should be noted that the method applies to two-dimensional flows behind circular cylinders in the low Reynolds number regimes ($100 < Re < 1250$).

REFERENCES

- Antonia, R. A. and S. Rajagopalan (1990). Determination of drag of a circular cylinder. *AIAA Journal* 28(10), 1833-1834.
- Bohl, D. G. and M. M. Koochesfahani (2009). MTV measurements of the vortical field in the wake of an airfoil oscillating at high reduced frequency. *Journal of Fluid Mechanics* 620, 63-88.
- Brennan, J. C., D. J. Fairhurst, R. H. Morris, G. McHale and M. I. Newton (2014). Investigation of the drag reducing effect of hydrophobized sand on cylinders. *Journal of Physics D: Applied Physics* 47(20), 205302.
- Cao, S., S. Ozono, Y. Tamura, Y. Ge and H. Kikugawa (2010). Numerical simulation of Reynolds number effects on velocity shear flow around a circular cylinder. *Journal of Fluids and Structures* 26(5), 685-702.
- Dimotakis, P. E. (1977). Laser Doppler velocimetry momentum defect measurements of cable drag at low to moderate Reynolds numbers. *NCBC Report, ContractNo: N62583/77-M-R541*.
- Feng, L. H. and J. J. Wang (2012). Synthetic jet control of separation in the flow over a circular cylinder. *Experiments in fluids* 53(2), 467-480.
- Goodfellow, S. D., S. Yarusevych and P. E. Sullivan (2012). Momentum coefficient as a parameter for aerodynamic flow control with synthetic jets. *AIAA Journal* 51(3), 623-631.
- He, G. S., N. Li and J. J. Wang (2014). Drag reduction of square cylinders with cut-corners at the front edges. *Experiments in Fluids* 55(6), 1-11.
- Henderson, R. D. (1995). Details of the drag curve near the onset of vortex shedding. *Physics of Fluids* 7(9), 2102-2104.
- Jordan, S. K. and J. E. Fromm (1972). Oscillatory drag, lift, and torque on a circular cylinder in a uniform flow. *Physics of Fluids* 15(3), 371-376.
- Konstantinidis, E. and S. Balabani (2007). Symmetric vortex shedding in the near wake of a circular cylinder due to streamwise perturbations. *Journal of Fluids and Structures* 23(7), 1047-1063.
- Sharma, S. D. and P. J. Deshpande (2012). Kutta-Joukowski theorem in viscous and unsteady flow. *Experiments in Fluids* 52(6), 1581-1591.
- Townsend, A. A. (1980). *The Structure of Turbulent Shear Flow*. Cambridge University Press.
- Van Oudheusden, B. W. (2013). PIV-based pressure measurement. *Measurement Science and Technology* 24(3), 032001.
- Wen, C. Y., C. L. Yeh, M. J. Wang and C. Y. Lin (2004). On the drag of two-dimensional flow about a circular cylinder. *Physics of Fluids* 16(10), 3828-3831.

Wieselsberger C. (1922). New data on the laws of fluid resistance, Tech. rep.,NACA TN-84.

Zdravkovich, M. M. (1997). *Flow Around Circular Cylinders, vol. 1. Fundamentals*. Oxford University Press.

Zhou, Y., M. M. Alam, H. X. Yang, H. Guo and D. H. Wood (2011). Fluid forces on a very low Reynolds number airfoil and their prediction. *International Journal of Heat and Fluid Flow* 32(1), 329-339.